Direct vagus nerve stimulation: A new tool to control allergic airway inflammation through α7 nicotinic acetylcholine receptor

Caroline Sévoz-Couche[1], Wupeng Liao[2], Hazel Yu Ci Foo[2], Isabelle Bonne[2], Lu Thong Beng[2], Caris Tan Qi Hui[3], Wendy Yen Xian Peh[4], Shih-Cheng Yen[4], and Wai Shui Fred Wong[2]

[1]UMR1158
[2]National University of Singapore Yong Loo Lin School of Medicine
[3]National University of Singapore - Kent Ridge Campus
[4]National University of Singapore

March 8, 2023

Abstract

Background and Purpose Asthma is characterized by airway inflammation, mucus hypersecretion and airway hyperresponsiveness (AHR). The activation of cholinergic anti-inflammatory pathway (CAP) through nicotinic agents has been shown to control experimental asthma. Yet, the effects of vagus nerve stimulation (VNS)-induced CAP on allergic inflammation remain unknown. Experimental Approach BALB/c mice were sensitized and challenged with house dust mite (HDM) extract, and treated with active VNS (5Hz, 0.5 ms, 0.1 mA). Bronchoalveolar lavage (BAL) fluid was assessed for total and differential cell counts and cytokine levels. Lungs were examined by histopathology and electron microscopy. AHR in response to methacholine was also measured. Key Results In the HDM mouse asthma model, active but not sham VNS reduced BAL fluid total and differential cell counts, blocked mucus hypersecretion and suppressed choline acetyltransferase (ChAT) expression in bronchial epithelial cells. Besides, active VNS also abated HDM-induced elevation of type 2 cytokines IL-4 and IL-5. Furthermore, goblet cell hyperplasia and collagen deposition were diminished in VNS-treated mice. Mechanistically, VNS was found to block the phosphorylation of transcription factor STAT6 and the level of IRF4 in total lung lysates. Finally, VNS abrogated methacholine-induced AHR in asthma mice. Therapeutic effects of VNS were abolished by prior administration with α-bungarotoxin, a specific inhibitor of α7 nicotinic receptors (α7nAChR). Conclusion Our data revealed the protective effects of VNS on various clinical features in allergic airway inflammation model. VNS, a clinically approved therapy for depression and epilepsy, appears to be a promising new strategy for controlling allergic asthma through α7nAChR.

Direct vagus nerve stimulation: A new tool to control allergic airway inflammation through α7 nicotinic acetylcholine receptor

Caroline Sevoz-Couche[1,2,*], Wupeng Liao[2,3], Hazel Y.C. Foo[2,3], Isabelle Bonne[4,5], Lu Thing Beng[4,5], Caris Tan Qi Hui[6], Wendy Yen Xian Peh[7,8], Shi-Cheng Yen[7,8], W.S. Fred Wong[2,3,9*]

[1]Sorbonne Universite, INSERM, UMRS1158 Neurophysiologie Respiratoire et Clinique, F-75005 Paris, France

[2]Department of Pharmacology, Yong Loo Lin School of Medicine, National University of Singapore, Singapore

[3]Singapore-HUJ Alliance for Research and Enterprise (SHARE), National University of Singapore, Singapore

[4]Electron Microscopy Unit, Yong Loo Lin School of Medicine, National University of Singapore, Singapore

[5]Department of Microbiology & Immunology, Yong Loo Lin School of Medicine, National University of Singapore, Singapore

[6]Advanced imaging and Histology Core, Immunology Program, Life Science Institute, National University of Singapore, Singapore

[7]The N.1 Institute for Health, National University of Singapore, Singapore

[8]Department of Electrical and Computer Engineering, National University of Singapore, Singapore

[9]Drug Discovery and Optimization Platform, Yong Loo Lin School of Medicine, National University of Singapore, Singapore

*Corresponding authors:

Caroline Sevoz-Couche

UMRS1158, Neurophysiologie Respiratoire et Clinique, Sorbonne Universite, Paris, France

E-mail : caroline.sevoz-couche@sorbonne-universite.fr

and

W.S. Fred Wong

Department of Pharmacology, Yong Loo Lin School of Medicine, National University of Singapore, Singapore 117600

E-mail: phcwongf@nus.edu.sg

Keywords

Asthma, vagus nerve stimulation, nicotinic receptors, bronchoalveolar inflammation

Bullet points

What is already known

- The “Cholinergic Anti-inflammatory Pathway” (CAP) reflexively monitors inflammatory responses by inhibiting pro-inflammatory cytokine synthesis
- Exogenous ACh, by binding to α7 nicotinic acetylcholine receptor (α7nAChR), was found to attenuate allergic airway inflammation

What this study adds

- Electrical vagus nerve stimulation (VNS) reduces airway inflammation and hyperesponsiveness in a mouse asthma model
- The protective effect of VNS on airway alteration involves α7nAChRs

Clinical significance

- VNS is a novel strategy for asthma management, especially for severe asthma and steroid-resistant asthma.

Abstract

Background and Purpose Asthma is characterized by airway inflammation, mucus hypersecretion and airway hyperresponsiveness (AHR). The activation of cholinergic anti-inflammatory pathway (CAP) through nicotinic agents has been shown to control experimental asthma. Yet, the effects of vagus nerve stimulation (VNS)-induced CAP on allergic inflammation remain unknown.

Experimental Approach BALB/c mice were sensitized and challenged with house dust mite (HDM) extract, and treated with active VNS (5Hz, 0.5 ms, 0.1 mA). Bronchoalveolar lavage (BAL) fluid was assessed for total and differential cell counts and cytokine levels. Lungs were examined by histopathology and electron microscopy. AHR in response to methacholine was also measured.

Key Results In the HDM mouse asthma model, active but not sham VNS reduced BAL fluid total and differential cell counts, blocked mucus hypersecretion and suppressed choline acetyltransferase (ChAT) expression in bronchial epithelial cells. Besides, active VNS also abated HDM-induced elevation of type 2 cytokines IL-4 and IL-5. Furthermore, goblet cell hyperplasia and collagen deposition were diminished in VNS-treated mice. Mechanistically, VNS was found to block the phosphorylation of transcription factor STAT6 and expression level of IRF4 in total lung lysates. Finally, VNS abrogated methacholine-induced AHR in asthma mice. Therapeutic effects of VNS were abolished by prior administration with α-bungarotoxin, a specific inhibitor of α7 nicotinic receptors (α7nAChR).

Conclusion and implications Our data revealed the protective effects of VNS on various clinical features in allergic airway inflammation model. VNS, a clinically approved therapy for depression and epilepsy, appears to be a promising new strategy for controlling allergic asthma.

Introduction

Asthma, one of the most common chronic inflammatory airway diseases, is estimated to affect some 339 million people worldwide(Ellwood et al., 2017). It is characterized by airway inflammation, mucus hypersecretion, collagen production, and airway hyperresponsiveness (AHR)(Page et al., 2016). These pathological features are caused by the infiltration of eosinophils and macrophages, increased production of pro-inflammatory mediators including Th2 cytokines IL-4, IL-5 and IL-13, and elevation of serum lgE level(Foster et al., 2017; Matucci et al., 2018; Schatz and Rosenwasser, 2014). The mainstay therapy for asthma consisting inhaled long-acting β_2-agonist (LABA) and inhaled corticosteroid (ICS) is able to control asthma symptoms in majority of asthmatics(Beasley et al., 2019). However, patients with severe asthma, accounting for approximately 10% of all asthma, often respond poorly to ICS and require add-on therapies like long-acting muscarinic antagonist (LAMA), leukotriene modifiers or biologics for full control of asthma symptoms. Unavoidably, patients are subject to increased risk of side effects(Holguin et al., 2020). As such, substantial effort has been made to discover novel anti-inflammatory strategies for asthma, especially for the severe asthma.

Acetylcholine (ACh) is synthesized from acetyl coenzyme A (acetyl-CoA) and choline by the action of choline acetyltransferase (ChAT)(Kistemaker et al., 2014). ACh acts by binding to two classes of cholinergic receptors: metabotropic muscarinic acetylcholine receptors (mAChRs) that are G protein-coupled receptors with seven transmembrane domains, and ionotropic nicotinic acetylcholine receptors (nAChRs) that are cation channels composed of a high diversity of subunits with two ACh binding sites(Wess et al., 2007). Stimulation of mAChRs is involved in airway smooth muscle contraction leading to AHR(Cazzola et al., 2021); whereas, activation of nAChRs is believed to possess anti-inflammatory actions(Wang et al., 2003). It has been shown that acute lung injury could be attenuated by a neuronal pathway

involving the release of ACh from the vagus nerve, which is known as the "Cholinergic Anti-inflammatory Pathway" (CAP). CAP reflexively monitors and adjusts inflammatory responses by inhibiting pro-inflammatory cytokine synthesis(Tracey, 2002; Wu et al., 2014). Resembling CAP activation, it has been shown that exogenous ACh or nicotine, by binding to α7 nicotinic acetylcholine receptor (α7nAChR), inhibited LPS-induced TNF-α production from macrophages(Wang et al., 2003). More recently, α7nAChR agonists like nicotine, PNU-22987 and GTS-21, or acetylcholinesterase inhibitor like neostigmine, were found to attenuate allergic airway inflammation(Antunes et al., 2020; Gahring et al., 2020; Mazloomi et al., 2018; Yamamoto et al., 2014; Yuan et al., 2021). Other than drug molecules, activation of CAP can also be achieved by non-drug approach such as pulsed electrical vagus nerve stimulation (VNS)(Giebelen et al., 2007; Ni et al., 2011; Su et al., 2007). VNS has been approved by the FDA as a therapy for refractory partial-onset epilepsy since 1997 and a therapy for treatment-resistant depression since 2005(Johnson and Wilson, 2018; Nemeroff et al., 2006). VNS has been demonstrated to be an effective anti-inflammatory therapy in inflammatory disease models such as endotoxin-induced systemic inflammation(Borovikova et al., 2000), inflammatory bowel disease(Bonaz et al., 2016) and rheumatoid arthritis(Koopman et al., 2016). While VNS was found to be effective in alleviating histamine-induced acute bronchoconstriction in animal models(Hoffmann et al., 2009) and in acute asthma exacerbations in patients unresponsive to initial standard care treatment(Miner et al., 2012) the potential effect of VNS on allergic airway inflammation has not been evaluated.

The purpose of the present study was to investigate whether VNS could protect against allergic airway inflammation in a house dust mite (HDM)-induced mouse asthma model. Our findings revealed for the first time that VNS attenuated allergic airway inflammation in a HDM asthma

model by suppressing type 2 immune responses and transcriptional activity of STAT6 and IRF-4 *via* the engagement of α7nAChR.

Methods

Animals

Female BALB/c mice of 6 to 8 weeks old were purchased from the InVivos Pte. Ltd. (Singapore) and maintained in a 12 h light-dark cycle with food and water available ad libitum. All experimental protocols were granted approval and performed according to the guidelines of the Institutional Animal Care and Use Committee (IACUC) of the National University of Singapore (Animal protocol number: R20-01056). Animal studies are reported in compliance with the ARRIVE guidelines(Percie du Sert et al., 2018) and with the recommendations made by the British Journal of Pharmacology(Lilley et al., 2020).

HDM-induced allergic airway inflammation in mice

The mouse asthma model was developed as previously described (Chan et al., 2016; Peh et al., 2015). Briefly, mice were anesthetized with isoflurane and then given 50 μg HDM (*Dermatophagoides pteronyssinus* extract, Greer Laboratories, Lenoir, NC) in 40 μl saline or 40 μl saline alone as a negative control, on days 0, 7, and 14 *via* the intratracheal (i.t.) route (Fig. 1).

VNS

VNS was delivered on day 14 under isofluorane anesthesia with hook-shaped electrodes that were coated with platinum-iridium wires (0.005″ bare, 0.008″ coated), with a distance of about 0.5 mm between hook electrode leads. The electrode was surgically placed around the mid-section of the left vagus nerve(Sévoz-Couche et al., 2002) (Fig. 1), to minimize undue effects on the heart(Pelleg et al., 1993). An isolated stimulator (Model 4100, A-M Systems, Carlsborg, WA) was used to deliver biphasic rectangular pulses for VNS. As high-frequency (>10 Hz) and/or high-intensity (>0.5 mA) VNS has chronotropic effects on the heart(Lee et al., 2018)

and broncho-constrictive effect on the airways(Watson et al., 1992) due to higher ACh release and stimulation of the mAChRs(Kawada et al., 2020), we used lower frequency (5 Hz) and intensity (0.1 mA) VNS. These parameters are known to produce anti-inflammatory effects through nAChR(Bernik et al., 2002; Boland et al., 2011; de Jonge et al., 2005) and prevent bronchoconstriction induced by histamine(Hoffmann et al., 2009). The phase widths of the biphasic pulses were 500 μs, with no interphase delay. VNS was applied 10 min before and 10 min after HDM i.t. administration, as performed in other acute inflammation models(Bernik et al., 2002; Komegae et al., 2018). After VNS, the wound was closed with permanent interrupted sutures, and the mice were under close observation until total recovery from anesthesia. Sham mice had similar surgery but were not stimulated. In a separate group of mice, intraperitoneal (i.p.) administration of α-bungarotoxin (α-BGTX, 1 μg/kg), a specific α7nACh receptor antagonist(Chen and Patrick, 1997), was performed 1 h before VNS or sham VNS(Kong et al., 2018). Mouse heart rate was monitored by electrocardiogram (ECG) to make sure it was stable and not modified by VNS (Supplementary Fig. 1).

Bronchoalveolar lavage (BAL) fluid, lung tissue and serum collection

Mice were sacrificed on day 17. BAL fluid, blood and lung tissue samples were collected and processed as previously described(Chan et al., 2016; Peh et al., 2015). Briefly, total blood was collected by cardiac puncture and serum was separated by centrifugation. Tracheotomy was performed, and a cannula was inserted into the trachea. Ice-cold PBS (0.5 ml × 3) was instilled into the lungs, and BAL fluid was collected. BAL fluid levels of IL-4 and IL-5 were measured using ELISA (BD Biosciences, Franklin Lakes, NJ). BAL fluid cells were pelleted, and the number of BAL fluid cells was determined using a hemocytometer. Differential cell types were analyzed by flow cytometry. Lung tissue was excised and stored at -80^{o}C for subsequent analysis.

Flow cytometry analysis

BAL fluid cells were stained via antibodies targeting surface makers CD45-PE/Cy7, CD11b-APC, Ly6G/6C-PerCP/Cy5.5, SiglecF-PE and CD11c-PB to differentiate total leukocytes, lymphocytes, alveolar macrophages (AMs), eosinophils and neutrophils as described previously(Chan et al., 2016). Leukocytes were identified as $CD45^+$, lymphocytes as $CD45^+SSC_{low}$, AMs as $CD45^+CD11c^+SiglecF^+$, eosinophils as $CD45^+CD11c^-SiglecF^+$, and neutrophils as $CD45^+Ly6G/6C^+CD11b^+$. The gating strategy for BAL fluid cells is shown in Supplemental Fig.2. All samples were run on BD LSRFortessa cell analyser and data were analysed with FlowJo software (BD Biosciences) or Cytobank (https://www.cytobank.org).

Histological analysis

Lungs were fixed in 10% neutral formalin, embedded with paraffin, cut into 5-μM sections, and stained with haematoxylin and eosin (H&E) for examining cell infiltration and with periodic acid-fluorescence Schiff (PAFS) for mucus production. Images were captured by Thunder Imaging System (Leica, Wetzlar, Germany). Scoring of H&E and PAFS staining was performed as described previously(Peh et al., 2015).

Transmission Electron Microscopy (TEM) Analysis

Lung tissues were fixed in 2.5% glutaraldehyde in PBS, washed three times in 0.1 M cacodylate buffer, and post-fixed in 1% buffered osmium for 1 h at room temperature. Lung samples were then dehydrated in ethanol and embedded in Araldite medium. Ultrathin sections were cut using an ultracut microtome (Leica) and stained with uranyl acetate and lead citrate. The stained lung sections were examined in a JEM 1400 transmission electron microscope operated at 100 kV and equipped with a Matataki Flash sCMOS camera (JEOL, Peabody, MA).

Immunofluorescence staining for ChAT

Lung tissues were fixed in 2% paraformaldehyde (PFA) + 30% sucrose fixative, and frozen in Tissue-Tek Optimum Cutting Temperature compound (Tissue-Tek OCT, Sakura Finetek, Torrance, CA) for 10-μm cryo-sectioning and subsequent immunofluorescence staining.

Briefly, tissue sections were incubated in 0.2% bovine serum albumin (BSA) blocking solution, followed by anti-ChAT primary antibody (rabbit monoclonal EPR 16590; Abcam, Cambridge, UK) incubation overnight at 4^{o}C, and by Cy3-conjugated anti-rabbit secondary antibody (Jackson ImmunoResearch Laboratories, Inc, West Grove, PA) to detect ChAT. FITC/AF488-conjugated anti-smooth muscle actin antibody (SMA, mouse clone 1A4; Sigma-Aldrich, St. Louis, MI) was used to identify airway smooth muscle cells. Sections were counterstained with 4,6-diamidino-2-phenylindole (DAPI) for cell nuclei visualization for histological analysis. A widefield fluorescence microscope (Axio Imager.Z1, Carl Zeiss MicroImaging, Inc., Jena, Germany) was used to view the specimens. Fiji (ImageJ) was used to analyze and quantify the fluorescence in the images obtained. Density was calculated as the mean of fluorescence in bronchial and peribronchial zones relative to total density, in 4 fields per lung section.

Immunoblotting

Total proteins from lung tissues were extracted in M-PER® Mammalian Protein Extraction Reagent containing protease and phosphatase inhibitors (Thermo Fisher Scientific, Waltham, MA). Total lung lysates were separated in 10% SDS-PAGE and immunoblots probed with anti-p-STAT6, anti-STAT6, and anti-IRF4 antibodies (Cell Signalling Technologies, Danvers, MA). β-actin (Proteintech, Rosemont, IL) was used as a loading control. Immunoblots were visualized and documented using ChemiDoc™ Touch Gel Imaging System (Bio-Rad Laboratories, Hercules, CA). Band intensity was quantitated using ImageJ software (NIH).

Measurements of AHR

Tracheotomy and intubation were performed as described previously (Peh et al., 2015). Trachea was intubated with a cannula that was connected to the Buxco Resistance and Compliance System (Data Sciences International, St. Paul, MN). Lung resistance (Rl) and dynamic compliance (Cdyn) in response to either saline or nebulized methacholine (2.5 - 20 mg/ml) were recorded and analysed using FinePointe software (Data Sciences

International). Results are expressed as a percentage of the respective basal values in response to PBS.

Statistical analysis

All data are expressed as mean ± SEM. One-way ANOVA of raw data without prior normalization followed by Dunnett's test was used to determine the significant differences between treatment groups with GraphPad PRISM (8.0.1). Two-way repeated ANOVA was performed for AHR analysis (factors: groups and methacholine doses). Comparisons of all groups vs HDM were performed (*), and specific comparison between HDM+VNS and HDM+VNS+ α-BGTX was also conducted (#).

Results

VNS attenuates HDM-induced airway inflammation through α7nAChR activation

Clusters of different immune cells including alveolar macrophages, eosinophils, lymphocytes and neutrophils from mouse BAL fluid were plotted by high-dimensional flow cytometry analysis based on surface markers (Fig. 2A). HDM challenge markedly increased the number of total inflammatory cells in BAL fluid, especially eosinophils and macrophages, as compared to saline (Fig.2B). VNS, but not sham VNS, prevented against HDM-induced inflammatory cell infiltration. Pre-treatment with α-BGTX, a specific α7nAChR antagonist, abrogated the anti-inflammatory effects of VNS (Fig. 2B). Concurrent ECG data showed that mouse heart rate was not affected by the VNS (Supplementary Fig. 1). Type 2 cytokines IL-4 and IL-5 in the BAL fluid were markedly elevated by HDM challenge. Active VNS drastically suppressed BAL fluid IL-4 and IL-5 levels, which were reversed by prior treatment with α-BGTX (Fig. 2C). HDM challenge induced bronchial epithelial hypertrophy as well as marked infiltration of inflammatory cells into the peribronchiolar and perivascular connective tissues (Fig. 2D). HDM challenge also promoted mucus hypersecretion in goblet cells, and VNS markedly

mitigated HDM-induced goblet cell mucus hypersecretion (Fig. 2E). That beneficial effect of VNS was abolished by pre-treatment of α-BGTX.

VNS ameliorates HDM-induced airway remodeling through α7nAChR activation

In contrast to the predominant ciliated epithelial cells identified in saline-challenged mice, pseudostratified epithelial cells, hyperplasia of goblet cells with vacuoles containing electron lucent substance, and ciliated cells with dense vacuoles (mucus granules), were shown in the epithelial lumen from HDM-exposed mice using TEM (Fig. 3A). VNS, but not sham VNS, reduced goblet cell hyperplasia induced by HDM, and this protective effect of VNS was abolised by prior administration of α-BGTX (Fig. 3A). In addition, TEM also uncovered an increase in collagen bundles in lung tissues from mice challenged with HDM (Fig. 3B). VNS, but not sham VNS, was able to decrease HDM-induced collagen deposition, and prior administration of α-BGTX reversed that beneficial effect of VNS (Fig. 3B).

VNS down-regulates HDM-induced increases in ChAT in airway epithelial cells

Small airways expressing muscarinic receptors are involved in all stages of asthma pathophysiologic manifestation, including AHR(Cazzola et al., 2021). Both neuronal and non-neuronal cells such as bronchial epithelial cells can express ChAT to produce and release ACh(Proskocil et al., 2004). In response to inflammatory stimuli, epithelial cell-derived Ach, considering that the small airways are not innervated by extrinsic or intrinsic cholinergic neurons(Barnes, 2004; Koarai and Ichinose, 2018), can bind muscarinic receptors to promote AHR. ChAT expression has been shown to be up-regulated in an allergic asthma model(Liu et al., 2018). Upon HDM challenge, the fluorescent density of ChAT in bronchial epithelialium was markedly elevated (apical level) (Fig. 4). VNS abolished HDM-induced ChAT expression, but that effect was reversed by prior administration of α-BGTX (Fig. 4).

VNS inhibits type 2 transcription factors STAT6 and IRF-4

Classical type 2 cytokines IL-4 and IL-13 have been shown to orchestrate allergic airway inflammation and remodeling by promoting JAK1/STAT6 and interferon regulatory factor 4 (IRF-4) signaling pathways(Gao et al., 2013; Oh et al., 2010). HDM challenge phosphorylated and activated transcription factor STAT6 and increased IRF4 protein level in total lung lysates. VNS, but not sham VNS, suppressed HDM-induced phosphorylation of STAT6 and up-regulation of IRF-4 protein expression in total lung lysates (Fig. 5). The inhibitory effects of VNS on p-STAT6 and IRF-4 were abrogated by the pre-treatment with α-BGTX (Fig. 5).

VNS blocks HDM-induced AHR

Lung resistance (R_L) and dynamic compliance (C_{dyn}) are the two parameters to evaluate AHR in asthma in response to bronchoconstrictor like methacholine, a cholinergic agent acting on muscarinic receptors present in bronchial smooth muscles(Kim et al., 2014). HDM-challenged mice developed AHR characterized by high R_L and low C_{dyn}. VNS, but not sham VNS, effectively blocked the increase in R_l and enhanced the decrease in C_{dyn} upon HDM challenge (Fig. 6). The beneficial effects of VNS were eradicated by prior administration of α-BGTX (Fig. 6).

Discussion

The activation of CAP by using nicotine or specific agonists for α7nACh receptor has been shown to protect against airway inflammation in allergic asthma models(Antunes et al., 2020; Gahring et al., 2020; Mazloomi et al., 2018; Yuan et al., 2021). Here we showed for the first time that VNS can also attenuate HDM-induced allergic airway inflammation. In mice sensitized and challenged with aeroallergen HDM, active VNS reduced BAL fluid cell counts, suppressed pulmonary cell infiltration and mucus hypersecretion, and ameliorated AHR. Histological and TEM analyses revealed that VNS also inhibited eosinophil degranulation, goblet cell hyperplasia and collagen deposition. The mechanisms underlying its anti-inflammatory effects may be attributable to the blockade of type 2 cytokines IL-4 and IL-5,

activated STAT6 and IRF-4 signaling pathways, and ACh biosynthesis enzyme ChAT expression in the allergic airways. The beneficial effects of VNS could be abrogated by prior administration of α-BGTX, a specific inhibitor for α7nAChR, highlighting an essential role of α7nAChR activation in mediating anti-asthma actions of VNS.

In addition to controlling the classic physiological functions (e.g. heart rate, gastric motility, pupil constriction)(Beaumont et al., 2017; Lu et al., 2020; Morishita and Guth, 1986), vagus nerve is also implicated in immune modulation, and its stimulation leads to effective anti-inflammatory actions through a mechanism called CAP(Tracey, 2002). Upon stimulation, the parasympathetic vagus nerve releases ACh to the surrounding tissues and immune cells, particularly macrophages in targeted organs including the lungs, especially the alveoli(Fox et al., 1980; Hertweck and Hung, 1980). ACh released by the vagus nerve during CAP activation mainly binds to a specific α-bungarotoxin-sensitive nicotinic receptors such as α7nAChR(Basus et al., 1988). Residential alveolar macrophages, airway epithelial cells and other infiltrated immune cells express various levels of α7nAChR(Blanchet et al., 2007; Yang et al., 2014), contributing to the anti-inflammatory effects CAP exerted by ACh.

VNS not only attenuated HDM-induced allergic inflammation, but also ameliorated airway remodeling and mucus hypersecretion. We have shown here for the first time that ultra-structural changes were observed under TEM in HDM-exposed airways. As reported in the lungs of asthmatic patients(Shahana et al., 2005), cardinal features of HDM-challenged airways included apparition of secretory vesicles in Clara cells, which give rise to mucus-producing goblet cells, and the presence of disjointed cells and collagen bundles. VNS suppressed mucus hypersecretion as shown by PAFS staining, as well as reduced goblet cell hyperplasia and

mucus granules inside the cells as visualized by TEM. These data indicate that VNS is able to modulate both macro- and microscopic hallmarks of allergic airways.

Allergic asthma is characterized by elevation of type 2 cytokines including IL-4, IL-5, and IL-13. IL-5 is a key regulator of eosinophil migration, proliferation, maturation and survival(Garcia et al., 2013). IL-4 is crucially involved in Th2 cell differentiation, immunoglobulin (Ig) class switching to lgE and eosinophil trafficking(Pelaia et al., 2022). Binding of IL-4 to IL-4 receptor results in JAK1 phosphorylation, which in turn recruits and phosphorylates transcription factor STAT6 for subsequent nuclear translocation and activation of target genes including GATA-3, CRTH2, arginase 1, Fizz1 and so on, leading to allergic airway inflammation and remodeling(Oh et al., 2010). IRF4 is also one of the target genes controlled by STAT6, and functions as another important transcription factor that orchestrates type 2 immune responses in both M2 and Th2 cell polarization(Gao et al., 2013; Satoh et al., 2010). IRF4-deficient mice produced drastically less IL-4 and IL-5(Flutter and Nestle, 2013). Low frequency VNS has been shown to reduce IL-4 level in septic rats as such it improves multiple organ dysfunction and reverses immunosuppression of T lymphocytes(Ren et al., 2018). Another recent report has demonstrated that vagal-α7nAChR signaling is required for anti-inflammatory responses in the lungs during an influenza infection(Gao et al., 2021). In the present study, low frequency VNS blocked BAL fluid levels of IL-4 and IL-5, as well as STAT6 phosphorylation in airway inflammation through α7nAChR activation.

ChAT, the enzyme responsible for the biosynthesis of ACh(Kistemaker et al., 2014), has been shown to localize at the apical end of the bronchial epithelium(Kummer et al., 2006; Wessler and Kirkpatrick, 2008). The basal level of ChAT is low in these cells from healthy subjects(Kawashima et al., 2007), but it is markedly increased in patients with inflammatory

conditions such as chronic obstructive bronchitis(Reinheimer et al., 1998) and asthma(Liu et al., 2018). In the present study, we observed a higher expression of ChAT in bronchial epithelial cells in HDM-exposed mice. Epithelial cells-derived ACh may contribute to goblet cells hyperplasia, mucus hypersecretion, and even AHR(Gosens and Gross, 2018; Kistemaker et al., 2014) in HDM asthma mice. Low frequency VNS attenuated the HDM-induced increase in epithelial ChAT and methacholine-induced AHR through α7nAChR activation.

Conclusion

Taken altogether, our data have demonstrated for the first time that VNS, as a non-drug therapy, is equally effective in treating the hallmarks of allergic asthma as compared to pharmacological intervention with nicotine agonists. Although ACh is the primary neurotransmitter contained in vagal post-ganglionic parasympathetic fibers in the lung(Hummel et al., 2019), we cannot rule out that some of the beneficial effects obtained with VNS may involve the activation of sympathetic catecholaminergic or non-cholinergic non-adrenergic (NANC) vagal fibers, especially in AHR as they are known to reduce bronchoconstriction(Hoffmann et al., 2012; Krishnakumar et al., 2002). However, the fact that the administration of the specific α7nACh receptor antagonist α-BGTX blocked all effects induced by VNS strongly implicates that ACh is imperative not only for anti-inflammatory but also for anti-constrictive effects in the lung. Non-invasive VNS has already been approved by the FDA for the treatment of depression and epilepsy, and has also been proven to be effective in a clinical study to reduce asthma exacerbation(Miner et al., 2012). Thus, our findings support VNS as a novel and safe strategy for asthma management, especially for severe asthma and steroid-resistant asthma.

Acknowledgments

This research work was supported by a grant A-0006243-00-00 from the National Research Foundation (W.S.F.W), a seed grant A-0002851-00-00 from the NUHS (W.S.F.W.).

Conflict of interest

None

List of References

Antunes, G.L., Silveira, J.S., Kaiber, D.B., Luft, C., da Costa, M.S., Marques, E.P., Ferreira, F.S., Breda, R.V., Wyse, A.T.S., Stein, R.T., Pitrez, P.M., da Cunha, A.A., 2020. Cholinergic anti-inflammatory pathway confers airway protection against oxidative damage and attenuates inflammation in an allergic asthma model. J Cell Physiol 235, 1838–1849. https://doi.org/10.1002/jcp.29101

Barnes, P.J., 2004. Distribution of Receptor Targets in the Lung. Proceedings of the American Thoracic Society 1, 345–351. https://doi.org/10.1513/pats.200409-045MS

Basus, V.J., Billeter, M., Love, R.A., Stroud, R.M., Kuntz, I.D., 1988. Structural studies of .alpha.-bungarotoxin. 1. Sequence-specific proton NMR resonance assignments. Biochemistry 27, 2763–2771. https://doi.org/10.1021/bi00408a016

Beasley, R., Harper, J., Bird, G., Maijers, I., Weatherall, M., Pavord, I.D., 2019. Inhaled Corticosteroid Therapy in Adult Asthma. Time for a New Therapeutic Dose Terminology. Am J Respir Crit Care Med 199, 1471–1477. https://doi.org/10.1164/rccm.201810-1868CI

Beaumont, E., Campbell, R.P., Andresen, M.C., Scofield, S., Singh, K., Libbus, I., KenKnight, B.H., Snyder, L., Cantrell, N., 2017. Cervical vagus nerve stimulation augments spontaneous discharge in second- and higher-order sensory neurons in the rat nucleus of the solitary tract. Am J Physiol Heart Circ Physiol 313, H354–H367. https://doi.org/10.1152/ajpheart.00070.2017

Bernik, T.R., Friedman, S.G., Ochani, M., DiRaimo, R., Ulloa, L., Yang, H., Sudan, S., Czura, C.J., Ivanova, S.M., Tracey, K.J., 2002. Pharmacological stimulation of the cholinergic antiinflammatory pathway. J. Exp. Med. 195, 781–788.

Blanchet, M.-R., Langlois, A., Israël-Assayag, E., Beaulieu, M.-J., Ferland, C., Laviolette, M., Cormier, Y., 2007. Modulation of eosinophil activation in vitro by a nicotinic receptor agonist. J Leukoc Biol 81, 1245–1251. https://doi.org/10.1189/jlb.0906548

Boland, C., Collet, V., Laterre, E., Lecuivre, C., Wittebole, X., Laterre, P.-F., 2011. Electrical Vagus Nerve Stimulation and Nicotine Effects in Peritonitis-Induced Acute Lung Injury in Rats. Inflammation 34, 29–35. https://doi.org/10.1007/s10753-010-9204-5

Bonaz, B., Sinniger, V., Hoffmann, D., Clarençon, D., Mathieu, N., Dantzer, C., Vercueil, L., Picq, C., Trocmé, C., Faure, P., Cracowski, J.-L., Pellissier, S., 2016. Chronic vagus nerve stimulation in Crohn's disease: a 6-month follow-up pilot study. Neurogastroenterol. Motil. 28, 948–953. https://doi.org/10.1111/nmo.12792

Borovikova, L.V., Ivanova, S., Zhang, M., Yang, H., Botchkina, G.I., Watkins, L.R., Wang, H., Abumrad, N., Eaton, J.W., Tracey, K.J., 2000. Vagus nerve stimulation attenuates the systemic inflammatory response to endotoxin. Nature 405, 458–462. https://doi.org/10.1038/35013070

Cazzola, M., Calzetta, L., Matera, M.G., 2021. Long-acting muscarinic antagonists and small airways in asthma: Which link? Allergy 76, 1990–2001. https://doi.org/10.1111/all.14766

Chan, T.K., Loh, X.Y., Peh, H.Y., Tan, W.N.F., Tan, W.S.D., Li, N., Tay, I.J.J., Wong, W.S.F., Engelward, B.P., 2016. House dust mite–induced asthma causes oxidative damage and DNA double-strand breaks in the lungs. Journal of Allergy and Clinical Immunology 138, 84-96.e1. https://doi.org/10.1016/j.jaci.2016.02.017

Chen, D., Patrick, J.W., 1997. The α-Bungarotoxin-binding Nicotinic Acetylcholine Receptor from Rat Brain Contains Only the α7 Subunit. Journal of Biological Chemistry 272, 24024–24029. https://doi.org/10.1074/jbc.272.38.24024

de Jonge, W.J., van der Zanden, E.P., The, F.O., Bijlsma, M.F., van Westerloo, D.J., Bennink, R.J., Berthoud, H.-R., Uematsu, S., Akira, S., van den Wijngaard, R.M., Boeckxstaens, G.E., 2005. Stimulation of the vagus nerve attenuates macrophage activation by activating the Jak2-STAT3 signaling pathway. Nat Immunol 6, 844–851. https://doi.org/10.1038/ni1229

Ellwood, P., Asher, M.I., Billo, N.E., Bissell, K., Chiang, C.-Y., Ellwood, E.M., El-Sony, A., García-Marcos, L., Mallol, J., Marks, G.B., Pearce, N.E., Strachan, D.P., 2017. The Global Asthma Network rationale and methods for Phase I global surveillance: prevalence, severity, management and risk factors. Eur Respir J 49, 1601605. https://doi.org/10.1183/13993003.01605-2016

Flutter, B., Nestle, F.O., 2013. What on "Irf" Is This Gene 4? Irf4 Transcription-Factor-Dependent Dendritic Cells Are Required for T Helper 2 Cell Responses in Murine Skin. Immunity 39, 625–627. https://doi.org/10.1016/j.immuni.2013.09.008

Foster, P.S., Maltby, S., Rosenberg, H.F., Tay, H.L., Hogan, S.P., Collison, A.M., Yang, M., Kaiko, G.E., Hansbro, P.M., Kumar, R.K., Mattes, J., 2017. Modeling T_H2 responses and airway inflammation to understand fundamental mechanisms regulating the pathogenesis of asthma. Immunol Rev 278, 20–40. https://doi.org/10.1111/imr.12549

Fox, B., Bull, T.B., Guz, A., 1980. Innervation of alveolar walls in the human lung: an electron microscopic study. J Anat 131, 683–692.

Gahring, L.C., Myers, E.J., Rogers, S.W., 2020. Inhaled aerosolized nicotine suppresses the lung eosinophilic response to house dust mite allergen. Am J Physiol Lung Cell Mol Physiol 319, L683–L692. https://doi.org/10.1152/ajplung.00227.2020

Gao, Y., Nish, S.A., Jiang, R., Hou, L., Licona-Limón, P., Weinstein, J.S., Zhao, H., Medzhitov, R., 2013. Control of T Helper 2 Responses by Transcription Factor IRF4-Dependent Dendritic Cells. Immunity 39, 722–732. https://doi.org/10.1016/j.immuni.2013.08.028

Gao, Z.-W., Li, L., Huang, Y.-Y., Zhao, C.-Q., Xue, S.-J., Chen, J., Yang, Z.-Z., Xu, J.-F., Su, X., 2021. Vagal-α7nAChR signaling is required for lung anti-inflammatory responses and arginase 1 expression during an influenza infection. Acta Pharmacol Sin 42, 1642–1652. https://doi.org/10.1038/s41401-020-00579-z

Garcia, G., Taille, C., Laveneziana, P., Bourdin, A., Chanez, P., Humbert, M., 2013. Anti-interleukin-5 therapy in severe asthma. European Respiratory Review 22, 251–257. https://doi.org/10.1183/09059180.00004013

Giebelen, I.A.J., van Westerloo, D.J., LaRosa, G.J., de Vos, A.F., van der Poll, T., 2007. LOCAL STIMULATION OF α7 CHOLINERGIC RECEPTORS INHIBITS LPS-INDUCED TNF-α RELEASE IN THE MOUSE LUNG. Shock 28, 700–703. https://doi.org/10.1097/shk.0b013e318054dd89

Gosens, R., Gross, N., 2018. The mode of action of anticholinergics in asthma. Eur Respir J 52, 1701247. https://doi.org/10.1183/13993003.01247-2017

Hertweck, M.S., Hung, K.-S., 1980. Ultrastructural evidence for the innervation of human pulmonary alveoli. Experientia 36, 112–113. https://doi.org/10.1007/BF02004006

Hoffmann, T.J., Mendez, S., Staats, P., Emala, C.W., Guo, P., 2009. Inhibition of Histamine-Induced Bronchoconstriction in Guinea Pig and Swine by Pulsed Electrical Vagus Nerve Stimulation. Neuromodulation: Technology at the Neural Interface 12, 261–269. https://doi.org/10.1111/j.1525-1403.2009.00234.x

Hoffmann, T.J., Simon, B.J., Zhang, Y., Emala, C.W., 2012. Low voltage vagal nerve stimulation reduces bronchoconstriction in guinea pigs through catecholamine release. Neuromodulation 15, 527–536. https://doi.org/10.1111/j.1525-1403.2012.00454.x

Holguin, F., Cardet, J.C., Chung, K.F., Diver, S., Ferreira, D.S., Fitzpatrick, A., Gaga, M., Kellermeyer, L., Khurana, S., Knight, S., McDonald, V.M., Morgan, R.L., Ortega, V.E., Rigau, D., Subbarao, P., Tonia, T., Adcock, I.M., Bleecker, E.R., Brightling, C., Boulet, L.-P., Cabana, M., Castro, M., Chanez, P., Custovic, A., Djukanovic, R., Frey, U., Frankemölle, B., Gibson, P., Hamerlijnck, D., Jarjour, N., Konno, S., Shen, H., Vitary, C., Bush, A., 2020. Management of severe asthma: a European Respiratory Society/American Thoracic Society guideline. Eur Respir J 55, 1900588. https://doi.org/10.1183/13993003.00588-2019

Hummel, J.P., Mayse, M.L., Dimmer, S., Johnson, P.J., 2019. Physiologic and histopathologic effects of targeted lung denervation in an animal model. Journal of Applied Physiology 126, 67–76. https://doi.org/10.1152/japplphysiol.00565.2018

Johnson, R.L., Wilson, C.G., 2018. A review of vagus nerve stimulation as a therapeutic intervention. JIR Volume 11, 203–213. https://doi.org/10.2147/JIR.S163248

Kawada, T., Sonobe, T., Nishikawa, T., Hayama, Y., Li, M., Zheng, C., Uemura, K., Akiyama, T., Pearson, J.T., Sugimachi, M., 2020. Contribution of afferent pathway to vagal nerve stimulation-induced myocardial interstitial acetylcholine release in rats. American Journal of Physiology-Regulatory, Integrative and Comparative Physiology 319, R517–R525. https://doi.org/10.1152/ajpregu.00080.2020

Kawashima, K., Yoshikawa, K., Fujii, Y.X., Moriwaki, Y., Misawa, H., 2007. Expression and function of genes encoding cholinergic components in murine immune cells. Life Sciences 80, 2314–2319. https://doi.org/10.1016/j.lfs.2007.02.036

Kim, M.-H., Song, W.-J., Kim, T.-W., Jin, H.-J., Sin, Y.-S., Ye, Y.-M., Kim, S.-H., Park, H.-W., Lee, B.-J., Park, H.-S., Yoon, H.-J., Choi, D.-C., Min, K.-U., Cho, S.-H., 2014. Diagnostic properties of the methacholine and mannitol bronchial challenge tests: A comparison study: Methacholine vs mannitol challenge test. Respirology 19, 852–856. https://doi.org/10.1111/resp.12334

Kistemaker, L.E.M., Bos, S.T., Mudde, W.M., Hylkema, M.N., Hiemstra, P.S., Wess, J., Meurs, H., Kerstjens, H.A.M., Gosens, R., 2014. Muscarinic M_3 Receptors Contribute to Allergen-Induced Airway Remodeling in Mice. Am J Respir Cell Mol Biol 50, 690–698. https://doi.org/10.1165/rcmb.2013-0220OC

Koarai, A., Ichinose, M., 2018. Possible involvement of acetylcholine-mediated inflammation in airway diseases. Allergology International 67, 460–466. https://doi.org/10.1016/j.alit.2018.02.008

Komegae, E.N., Farmer, D.G.S., Brooks, V.L., McKinley, M.J., McAllen, R.M., Martelli, D., 2018. Vagal afferent activation suppresses systemic inflammation via the splanchnic anti-inflammatory pathway. Brain, Behavior, and Immunity 73, 441–449. https://doi.org/10.1016/j.bbi.2018.06.005

Kong, W., Kang, K., Gao, Y., Liu, H., Meng, X., Cao, Y., Yang, S., Liu, W., Zhang, J., Yu, K., Zhao, M., 2018. GTS-21 Protected Against LPS-Induced Sepsis Myocardial Injury in Mice Through α7nAChR. Inflammation 41, 1073–1083. https://doi.org/10.1007/s10753-018-0759-x

Koopman, F.A., Chavan, S.S., Miljko, S., Grazio, S., Sokolovic, S., Schuurman, P.R., Mehta, A.D., Levine, Y.A., Faltys, M., Zitnik, R., Tracey, K.J., Tak, P.P., 2016. Vagus nerve stimulation inhibits cytokine production and attenuates disease severity in rheumatoid arthritis. Proc. Natl. Acad. Sci. U.S.A. 113, 8284–8289. https://doi.org/10.1073/pnas.1605635113

Krishnakumar, S., Holmes, E.P., Moore, R.M., Kappel, L., Venugopal, C.S., 2002. Non-adrenergic non-cholinergic excitatory innervation in the airways: role of neurokinin-2 receptors. Autonom & Auta Pharm 22, 215–224. https://doi.org/10.1046/j.1474-8673.2002.00262.x

Kummer, W., Wiegand, S., Akinci, S., Wessler, I., Schinkel, A.H., Wess, J., Koepsell, H., Haberberger, R.V., Lips, K.S., 2006. Role of acetylcholine and polyspecific cation transporters in serotonin-induced bronchoconstriction in the mouse. Respir Res 7, 65. https://doi.org/10.1186/1465-9921-7-65

Lee, S.W., Kulkarni, K., Annoni, E.M., Libbus, I., KenKnight, B.H., Tolkacheva, E.G., 2018. Stochastic vagus nerve stimulation affects acute heart rate dynamics in rats. PLoS One 13, e0194910. https://doi.org/10.1371/journal.pone.0194910

Lilley, E., Stanford, S.C., Kendall, D.E., Alexander, S.P.H., Cirino, G., Docherty, J.R., George, C.H., Insel, P.A., Izzo, A.A., Ji, Y., Panettieri, R.A., Sobey, C.G., Stefanska, B., Stephens, G., Teixeira, M., Ahluwalia, A., 2020. ARRIVE 2.0 and the British Journal of Pharmacology: Updated guidance for 2020. Br J Pharmacol 177, 3611–3616. https://doi.org/10.1111/bph.15178

Liu, D., Li, T., Luo, H., Zuo, X., Liu, S., Wu, S., 2018. The effect of the cholinergic anti-inflammatory pathway on collagen-induced arthritis involves the modulation of dendritic cell differentiation. Arthritis Res Ther 20, 263. https://doi.org/10.1186/s13075-018-1759-9

Lu, K.-H., Cao, J., Phillips, R., Powley, T.L., Liu, Z., 2020. Acute effects of vagus nerve stimulation parameters on gastric motility assessed with magnetic resonance imaging. Neurogastroenterol Motil 32, e13853. https://doi.org/10.1111/nmo.13853

Matucci, A., Vultaggio, A., Maggi, E., Kasujee, I., 2018. Is IgE or eosinophils the key player in allergic asthma pathogenesis? Are we asking the right question? Respir Res 19, 113. https://doi.org/10.1186/s12931-018-0813-0

Mazloomi, E., Ilkhanizadeh, B., Zare, A., Mohammadzadeh, A., Delirezh, N., Shahabi, S., 2018. Evaluation of the efficacy of nicotine in treatment of allergic asthma in BALB/c mice. Int Immunopharmacol 63, 239–245. https://doi.org/10.1016/j.intimp.2018.08.006

Miner, J.R., Lewis, L.M., Mosnaim, G.S., Varon, J., Theodoro, D., Hoffmann, T.J., 2012. Feasibility of percutaneous vagus nerve stimulation for the treatment of acute asthma exacerbations. Acad Emerg Med 19, 421–429. https://doi.org/10.1111/j.1553-2712.2012.01329.x

Morishita, T., Guth, P.H., 1986. Vagal nerve stimulation causes noncholinergic dilatation of gastric arterioles. Am J Physiol 250, G660-664. https://doi.org/10.1152/ajpgi.1986.250.5.G660

Nemeroff, C.B., Mayberg, H.S., Krahl, S.E., McNamara, J., Frazer, A., Henry, T.R., George, M.S., Charney, D.S., Brannan, S.K., 2006. Erratum: VNS Therapy in Treatment-Resistant Depression: Clinical Evidence and Putative Neurobiological Mechanisms. Neuropsychopharmacol 31, 2329–2329. https://doi.org/10.1038/sj.npp.1301190

Ni, Y.F., Tian, F., Lu, Z.F., Yang, G.D., Fu, H.Y., Wang, J., Yan, X.L., Zhao, Y.C., Wang, Y.J., Jiang, T., 2011. Protective Effect of Nicotine on Lipopolysaccharide-Induced Acute Lung Injury in Mice. Respiration 81, 39–46. https://doi.org/10.1159/000319151

Oh, C.K., Geba, G.P., Molfino, N., 2010. Investigational therapeutics targeting the IL-4/IL-13/STAT-6 pathway for the treatment of asthma. European Respiratory Review 19, 46–54. https://doi.org/10.1183/09059180.00007609

Page, C., O'Shaughnessy, B., Barnes, P., 2016. Pathogenesis of COPD and Asthma, in: Page, C.P., Barnes, P.J. (Eds.), Pharmacology and Therapeutics of Asthma and COPD, Handbook of Experimental Pharmacology. Springer International Publishing, Cham, pp. 1–21. https://doi.org/10.1007/164_2016_61

Peh, H.Y., Ho, W.E., Cheng, C., Chan, T.K., Seow, A.C.G., Lim, A.Y.H., Fong, C.W., Seng, K.Y., Ong, C.N., Wong, W.S.F., 2015. Vitamin E Isoform γ-Tocotrienol Downregulates House Dust Mite-Induced Asthma. J Immunol 195, 437–444. https://doi.org/10.4049/jimmunol.1500362

Pelaia, C., Heffler, E., Crimi, C., Maglio, A., Vatrella, A., Pelaia, G., Canonica, G.W., 2022. Interleukins 4 and 13 in Asthma: Key Pathophysiologic Cytokines and Druggable Molecular Targets. Front. Pharmacol. 13, 851940. https://doi.org/10.3389/fphar.2022.851940

Pelleg, A., Hurt, C.M., Soler-Baillo, J.M., Polansky, M., 1993. Electrophysiological-anatomic correlates of ATP-triggered vagal reflex in dogs. Am J Physiol 265, H681-690. https://doi.org/10.1152/ajpheart.1993.265.2.H681

Percie du Sert, N., Hurst, V., Ahluwalia, A., Alam, S., Altman, D.G., Avey, M.T., Baker, M., Browne, W., Clark, A., Cuthill, I.C., Dirnagl, U., Emerson, M., Garner, P., Howells, D.W., Karp, N.A., MacCallum, C.J., Macleod, M., Petersen, O., Rawle, F., Reynolds, P., Rooney, K., Sena, E.S., Silberberg, S.D., Steckler, T., Würbel, H., Holgate, S.T., 2018. Revision of the ARRIVE

guidelines: rationale and scope. BMJ Open Science 2. https://doi.org/10.1136/bmjos-2018-000002

Proskocil, B.J., Sekhon, H.S., Jia, Y., Savchenko, V., Blakely, R.D., Lindstrom, J., Spindel, E.R., 2004. Acetylcholine Is an Autocrine or Paracrine Hormone Synthesized and Secreted by Airway Bronchial Epithelial Cells. Endocrinology 145, 2498–2506. https://doi.org/10.1210/en.2003-1728

Reinheimer, T., Münch, M., Bittinger, F., Racké, K., Kirkpatrick, C.J., Wessler, I., 1998. Glucocorticoids mediate reduction of epithelial acetylcholine content in the airways of rats and humans. European Journal of Pharmacology 349, 277–284. https://doi.org/10.1016/S0014-2999(98)00185-X

Ren, C., Li, X.H., Wu, Y., Dong, N., Yao, Y.M., 2018. [Influence of vagus nerve on multiple organ function and immune reaction of T lymphocytes in septic rats]. Zhonghua Shao Shang Za Zhi 34, 815–820. https://doi.org/10.3760/cma.j.issn.1009-2587.2018.11.018

Satoh, T., Takeuchi, O., Vandenbon, A., Yasuda, K., Tanaka, Y., Kumagai, Y., Miyake, T., Matsushita, K., Okazaki, T., Saitoh, T., Honma, K., Matsuyama, T., Yui, K., Tsujimura, T., Standley, D.M., Nakanishi, K., Nakai, K., Akira, S., 2010. The Jmjd3-Irf4 axis regulates M2 macrophage polarization and host responses against helminth infection. Nat Immunol 11, 936–944. https://doi.org/10.1038/ni.1920

Schatz, M., Rosenwasser, L., 2014. The Allergic Asthma Phenotype. The Journal of Allergy and Clinical Immunology: In Practice 2, 645–648. https://doi.org/10.1016/j.jaip.2014.09.004

Sévoz-Couche, C., Hamon, M., Laguzzi, R., 2002. Antinociceptive effect of cardiopulmonary chemoreceptor and baroreceptor reflex activation in the rat. Pain 99, 71–81.

Shahana, S., Björnsson, E., Lúdvíksdóttir, D., Janson, C., Nettelbladt, O., Venge, P., Roomans, G.M., BHR-group, 2005. Ultrastructure of bronchial biopsies from patients with allergic and non-allergic asthma. Respir Med 99, 429–443. https://doi.org/10.1016/j.rmed.2004.08.013

Su, X., Lee, J.W., Matthay, Z.A., Mednick, G., Uchida, T., Fang, X., Gupta, N., Matthay, M.A., 2007. Activation of the α7 nAChR Reduces Acid-Induced Acute Lung Injury in Mice and Rats. Am J Respir Cell Mol Biol 37, 186–192. https://doi.org/10.1165/rcmb.2006-0240OC

Tracey, K.J., 2002. The inflammatory reflex. Nature 420, 853–859. https://doi.org/10.1038/nature01321

Wang, Hong, Yu, M., Ochani, M., Amella, C.A., Tanovic, M., Susarla, S., Li, J.H., Wang, Haichao, Yang, H., Ulloa, L., Al-Abed, Y., Czura, C.J., Tracey, K.J., 2003. Nicotinic acetylcholine receptor α7 subunit is an essential regulator of inflammation. Nature 421, 384–388. https://doi.org/10.1038/nature01339

Watson, N., Barnes, P.J., Maclagan, J., 1992. Actions of methoctramine, a muscarinic M2 receptor antagonist, on muscarinic and nicotinic cholinoceptors in guinea-pig airways in vivo and in vitro. British Journal of Pharmacology 105, 107–112. https://doi.org/10.1111/j.1476-5381.1992.tb14219.x

Wess, J., Eglen, R.M., Gautam, D., 2007. Muscarinic acetylcholine receptors: mutant mice provide new insights for drug development. Nat Rev Drug Discov 6, 721–733. https://doi.org/10.1038/nrd2379

Wessler, I., Kirkpatrick, C.J., 2008. Acetylcholine beyond neurons: the non-neuronal cholinergic system in humans. Br J Pharmacol 154, 1558–1571. https://doi.org/10.1038/bjp.2008.185

Wu, H., Li, L., Su, X., 2014. Vagus Nerve through α 7 nAChR Modulates Lung Infection and Inflammation: Models, Cells, and Signals. BioMed Research International 2014, 1–20. https://doi.org/10.1155/2014/283525

Yamamoto, T., Kodama, T., Lee, J., Utsunomiya, N., Hayashi, S., Sakamoto, H., Kuramoto, H., Kadowaki, M., 2014. Anti-allergic role of cholinergic neuronal pathway via α7 nicotinic ACh receptors on mucosal mast cells in a murine food allergy model. PLoS One 9, e85888. https://doi.org/10.1371/journal.pone.0085888

Yang, X., Zhao, C., Gao, Z., Su, X., 2014. A novel regulator of lung inflammation and immunity: pulmonary parasympathetic inflammatory reflex. QJM 107, 789–792. https://doi.org/10.1093/qjmed/hcu005

Yuan, F., Jiang, L., Li, Q., Sokulsky, L., Wanyan, Y., Wang, L., Liu, X., Zhou, L., Tay, H.L., Zhang, G., Yang, M., Li, F., 2021. A Selective α7 Nicotinic Acetylcholine Receptor Agonist, PNU-282987, Attenuates ILC2s Activation and Alternaria-Induced Airway Inflammation. Front. Immunol. 11, 598165. https://doi.org/10.3389/fimmu.2020.598165

Figure Legends

Figure 1. A schematic diagram for the development of HDM-induced airway inflammation model and VNS treatment protocol. At days 0 and 7, mice were anesthetized under isoflurane and sensitized via intra-tracheal (i.t.) administration of either saline or 50 μg HDM extract. On day 14, mice were challenged with the same dose of HDM, with (active VNS) or without (Sham VNS) electrical stimulation of the vagus nerve. Administration of α-bungarotoxin (α-BGTX) was given i.p. one hour before VNS. Mice were sacrificed on day 17.

Figure 2. VNS attenuates HDM-induced allergic airway inflammation. (A) Flow cytometry viSNE, showing BAL fluid macrophage, eosinophil, neutrophil and lymphocyte populations. Clusters were identified based on cell surface marker expressions as described in the Methods section. (B) Total and differential cell counts in mouse BAL fluid. (C) Lung sections stained with haematoxylin and eosin (H&E) with corresponding quantitative analysis. Scale: 100 μm. (D) Lung sections for mucus staining with Periodic Acid-Fluorescence Schiff (PAFS) solution with corresponding quantitative analysis. (E) Levels of cytokines IL-4 and IL-5 in BAL fluid were determined by ELISA.

Values are shown as means ± SEM of 5 mice. *Significant difference from saline: ***$p<0.001$, #$p<0.05$, ##$p<0.01$, and ###$p<0.001$.

Figure 3. VNS inhibits goblet cell hyperplasia and collagen deposition in HDM-induced allergic airway. (A) Representative TEM images of bronchial epithelium. Ciliated cells (Ci)

are recognized by its columnar shape, large basal nucleus, electron lucent cytoplasm and the presence of unaltered cilia. Non-ciliated Clara cells (C) are columnar-shaped with a large amount of cytoplasmic electron dense secretory granules beside the cell organelles. Goblet cells (G) are dome-shaped and identified by membrane-bound mucous granules containing electron lucent substance. In saline control mice, bronchial epithelium is regular, and mainly populated with Ci (black arrows). In HDM-challenged mice, numerous G (white arrows) and C appear, causing pseudostratification and hyperplasia, and Ci are compressed towards the side. In VNS- but not sham VNS-treated HDM mice, the number of secretory cells (G and C) was reduced, and that effect was reversed by i.p. administration of α-BGTX. (B) Representative TEM images of lung subepithelial area. Large collagen fibers (white arrows) are found in the lung subepithelial area of HDM-exposed mice. Collagen bundles are shown with higher magnification. In VNS- but not sham VNS-treated asthma mice, the apparition of collagen deposition was reduced. Prior administration of α-BGTX reversed the anti-fibrotic effect of VNS.

Figure 4. VNS down-regulates HDM-induced cholinergic acetyl transferase (ChAT) expression in peribronchiolar areas of the allergic airway. (A) Lung sections were stained for ChAT (red), smooth muscle actin (SMA, green), and DNA nuclear stain (DAPI, blue). Scale: 50 μm. (B) Quantification of fluorescent intensity of ChAT in peribronchiolar areas. Values are shown as means ± SEM of 5 animals. *Significant difference from saline: **p<0.01, #p< .05, and ##p<0.01.

Figure 5. VNS modulates HDM-induced transcription factors in allergic airway. (A) Representative immunoblots of phospho-STAT6 and total STAT6 in mouse total lung lysates with corresponding quantitative analysis. (B) Representative immunoblots of IRF-4 in mouse

total lung lysate with corresponding quantitative analysis. Values are shown as means ± SEM of 5 mice. *Significant difference from saline: **p<0.01, ***p<0.001, $^{\#}$p<0.05, $^{\#\#}$p<0.01, and $^{\#\#\#}$p<0.001.

Figure 6. VNS blocks HDM-induced airway hyperresponsiveness (AHR). AHR in response to increasing concentrations of aerosolized methacholine was measured on day 17. AHR is expressed as percentage change compared with the baseline (PBS) level of (A) lung resistance (R_L) and (B) dynamic compliance (C_{dyn}). Values are shown as means ± SEM of 5 mice. *Significant difference from saline: *p<0.05, **p<0.01, and $^{\#}$p< .05.

Supplementary Figures

Figure S1. Heart rate is not altered by VNS in HDM mice. Electrocardiogram (ECG) was recorded on Day 14, under isofluorane anaesthesia during VNS procedure before and after HDM. ECG was recorded using stainless steel pins placed subcutaneously in fore- and hind-paws. Signals were amplified and filtered (Universal Amplifier). The R wave of the ECG was discriminated with a window discriminator and used to generate pulses. ECG signals were imported to a computer running Spike 2 software (CED). Cardiac intervals and heart rate were automatically computed from R wave pulses (bin size: 1 s).

Figure S2. Gating strategy for BAL fluid inflammatory cells.

Figure 1

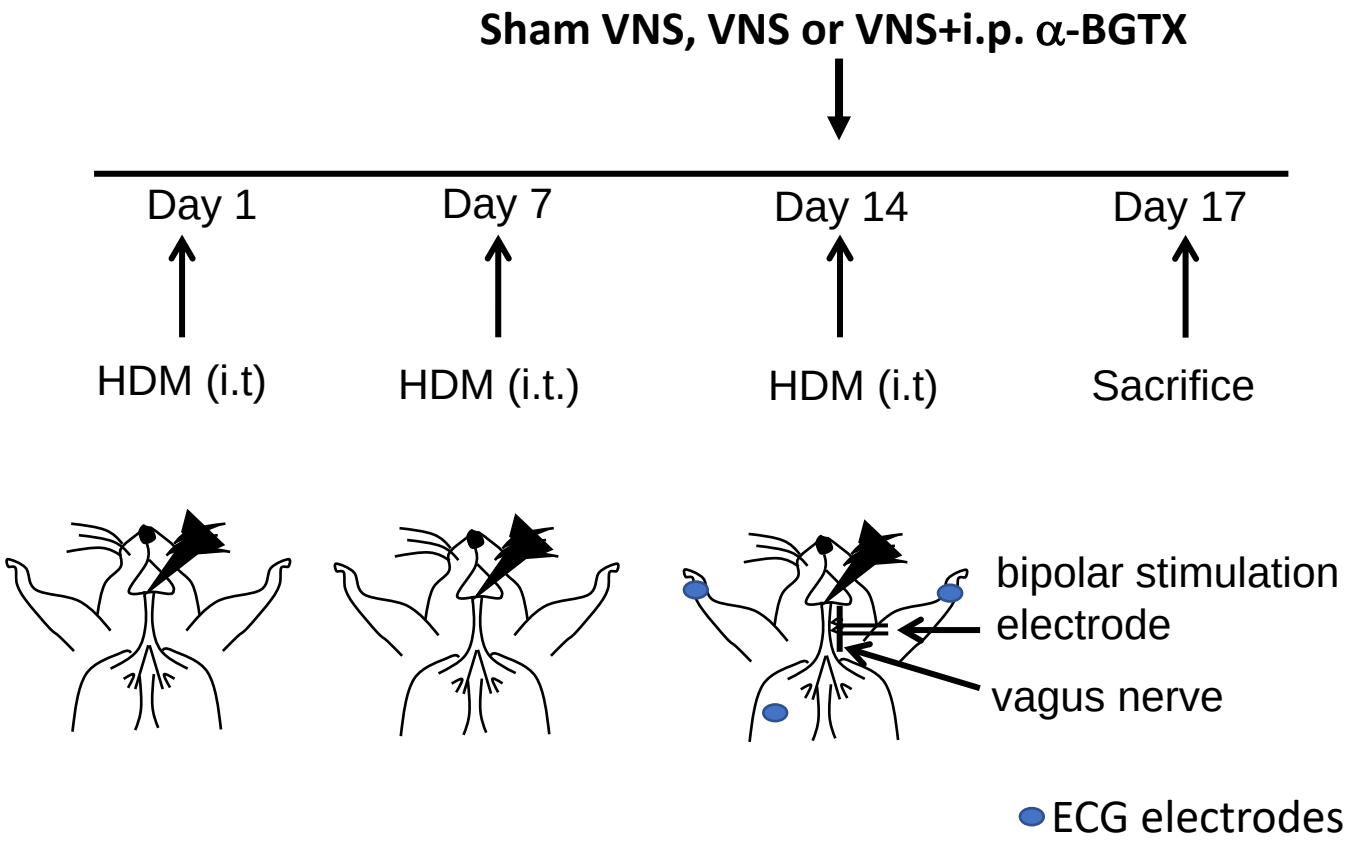
Sham VNS, VNS or VNS+i.p. α-BGTX
Day 1
Day 7
Day 14
Day 17
HDM (i.t)
HDM (i.t.)
HDM (i.t)
Sacrifice
bipolar stimulation electrode
vagus nerve
ECG electrodes

Figure 2

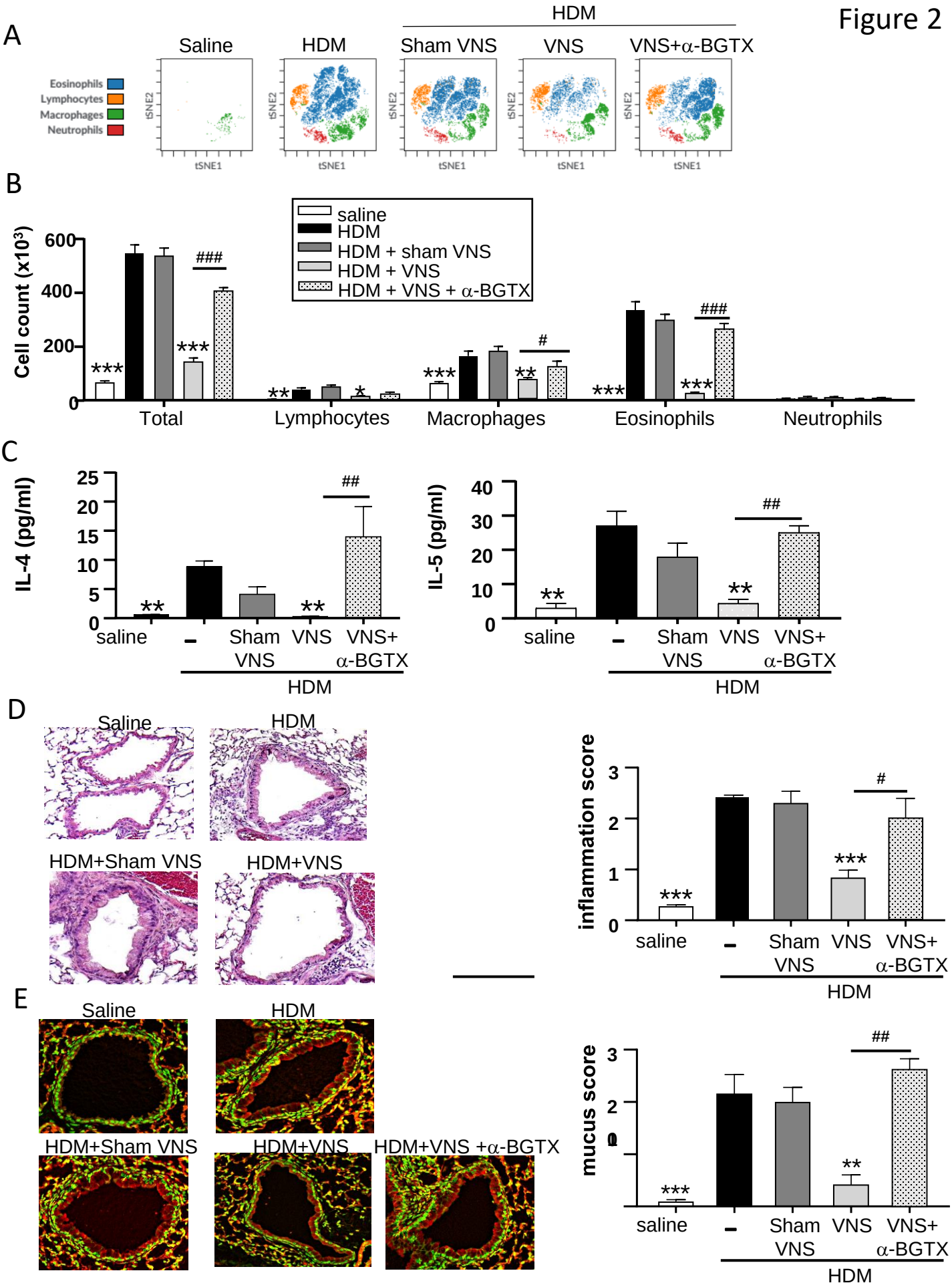
A
HDM
Saline
HDM
Sham VNS
VNS
VNS+α-BGTX
Eosinophils
Lymphocytes
Macrophages
Neutrophils
tSNE2
tSNE1
B
saline
HDM
HDM + sham VNS
HDM + VNS
HDM + VNS + α-BGTX
Cell count (x10³)
600
400
200
0
###
***
**
*
#
Total
Lymphocytes
Macrophages
Eosinophils
Neutrophils
C
IL-4 (pg/ml)
25
20
15
10
5
0
##
**
saline
–
Sham VNS
VNS
VNS+ α-BGTX
HDM
IL-5 (pg/ml)
40
30
20
10
0
D
Saline
HDM
HDM+Sham VNS
HDM+VNS
inflammation score
3
2
1
0
***
#
E
Saline
HDM
HDM+Sham VNS
HDM+VNS
HDM+VNS +α-BGTX
mucus score
3
2
1
0
***
**
##

Figure 3

A

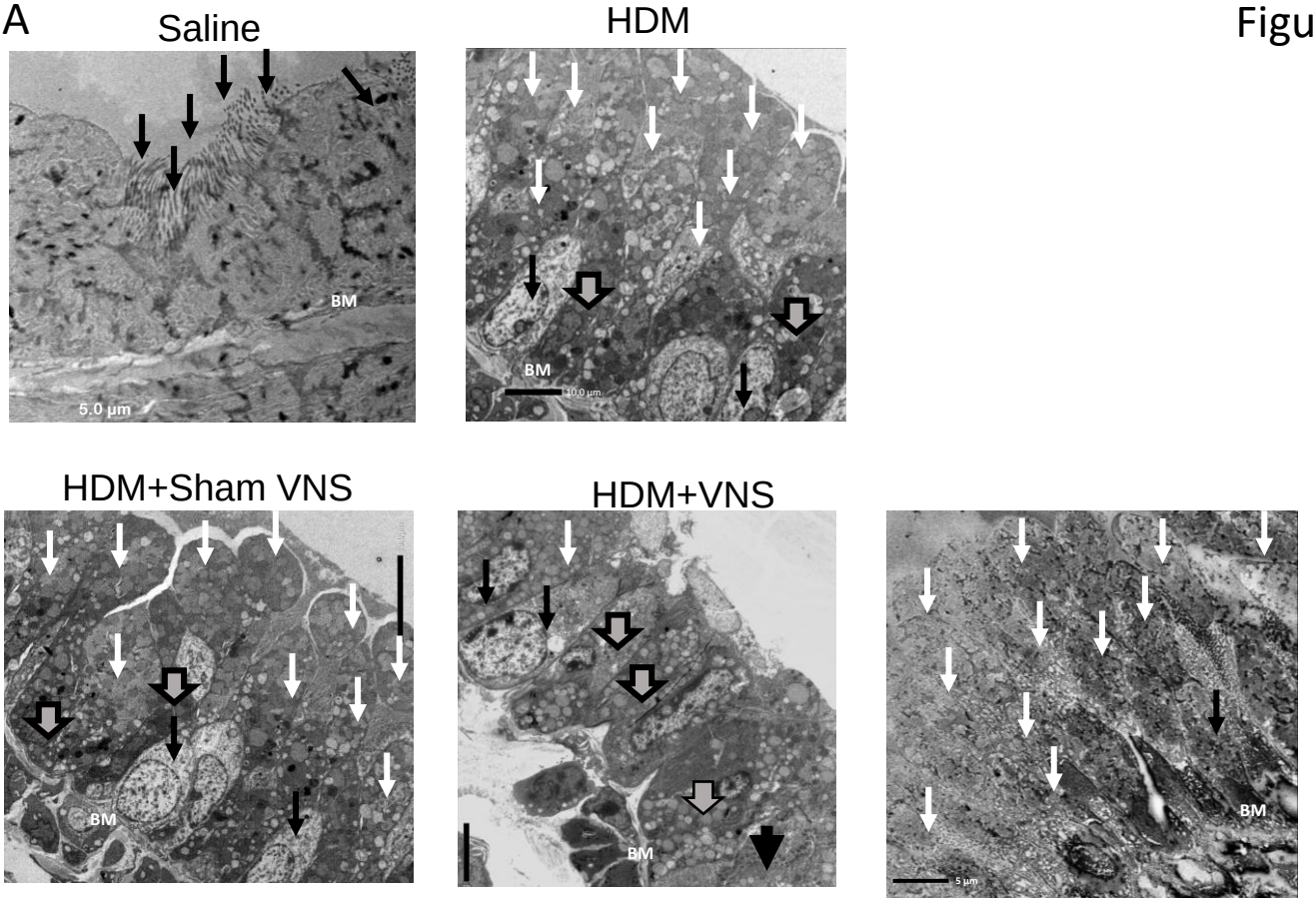
Saline
HDM
BM
5.0 µm
BM
10.0 µm
HDM+Sham VNS
HDM+VNS
BM
BM
BM
5 µm

B

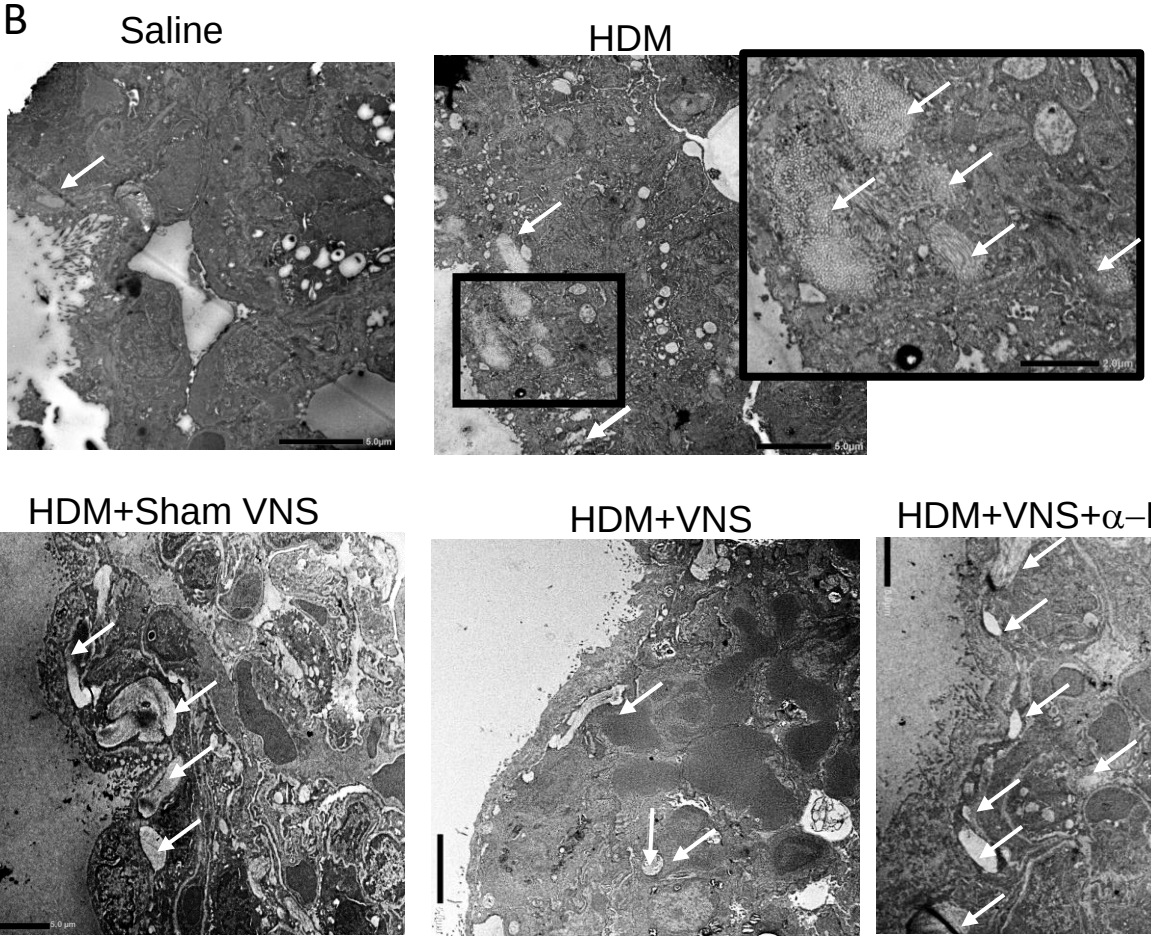
Saline
HDM
5.0µm
5.0µm
HDM+Sham VNS
HDM+VNS
HDM+VNS+α–BGTX
5.0 µm

A

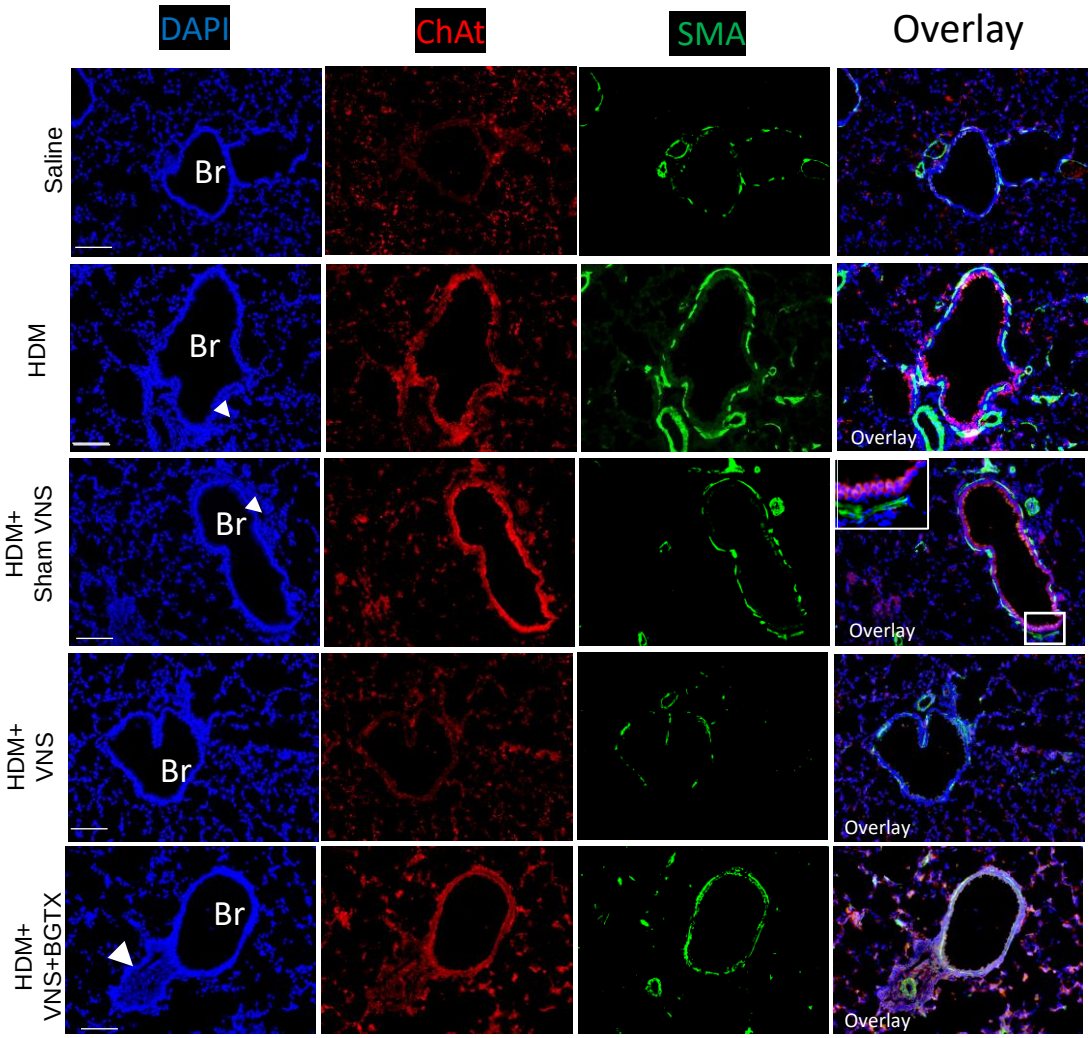
DAPI
ChAt
SMA
Overlay
Saline
HDM
HDM+ Sham VNS
HDM+ VNS
HDM+ VNS+BGTX
Br
Overlay

B

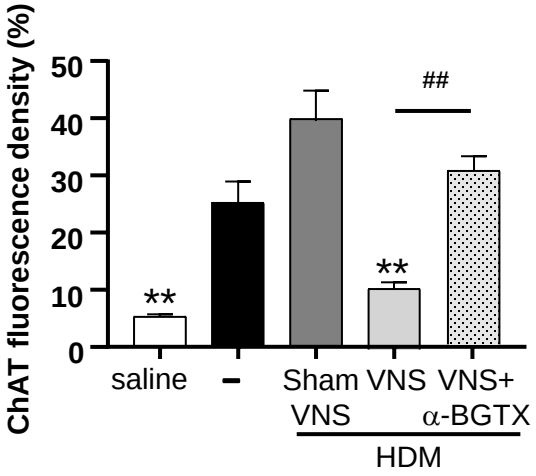
ChAT fluorescence density (%)
50
40
30
20
10
0
**
**
##
saline
–
Sham VNS
VNS+ α-BGTX
HDM

Figure 5

A

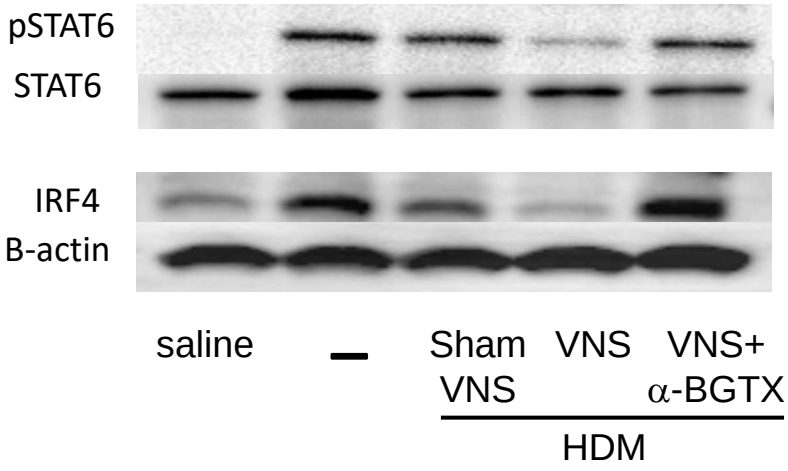
pSTAT6
STAT6
IRF4
B-actin
saline
–
Sham VNS
VNS
VNS+ α-BGTX
HDM

B

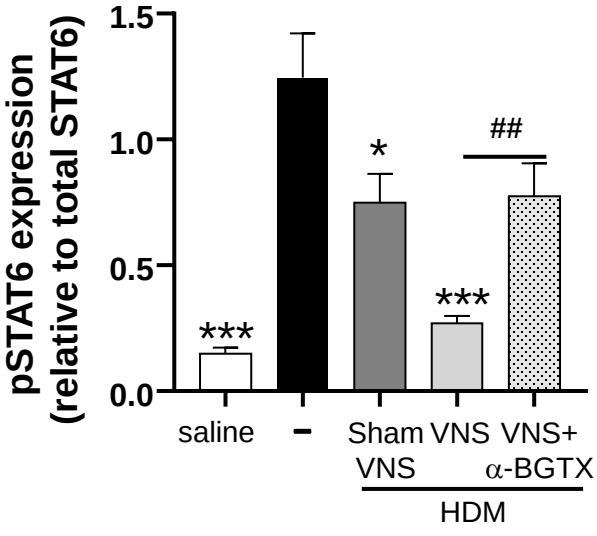
pSTAT6 expression (relative to total STAT6)
1.5
1.0
0.5
0.0
***
*
***
##
saline
–
Sham VNS
VNS
VNS+ α-BGTX
HDM

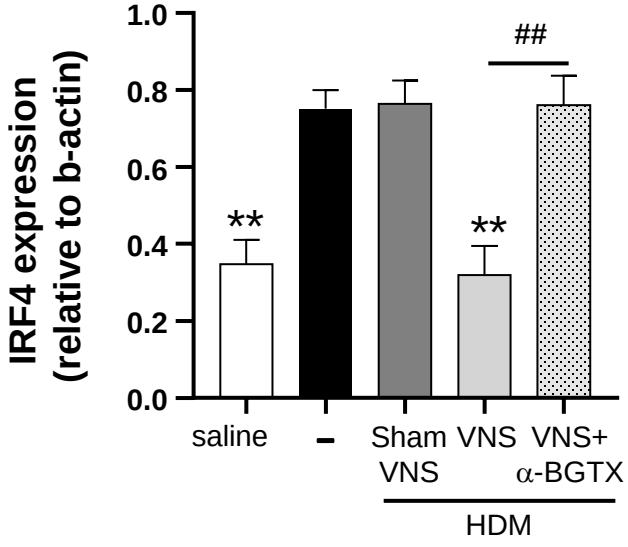
IRF4 expression (relative to b-actin)
1.0
0.8
0.6
0.4
0.2
0.0
**
**
##
saline
–
Sham VNS
VNS
VNS+ α-BGTX
HDM

Figure 6

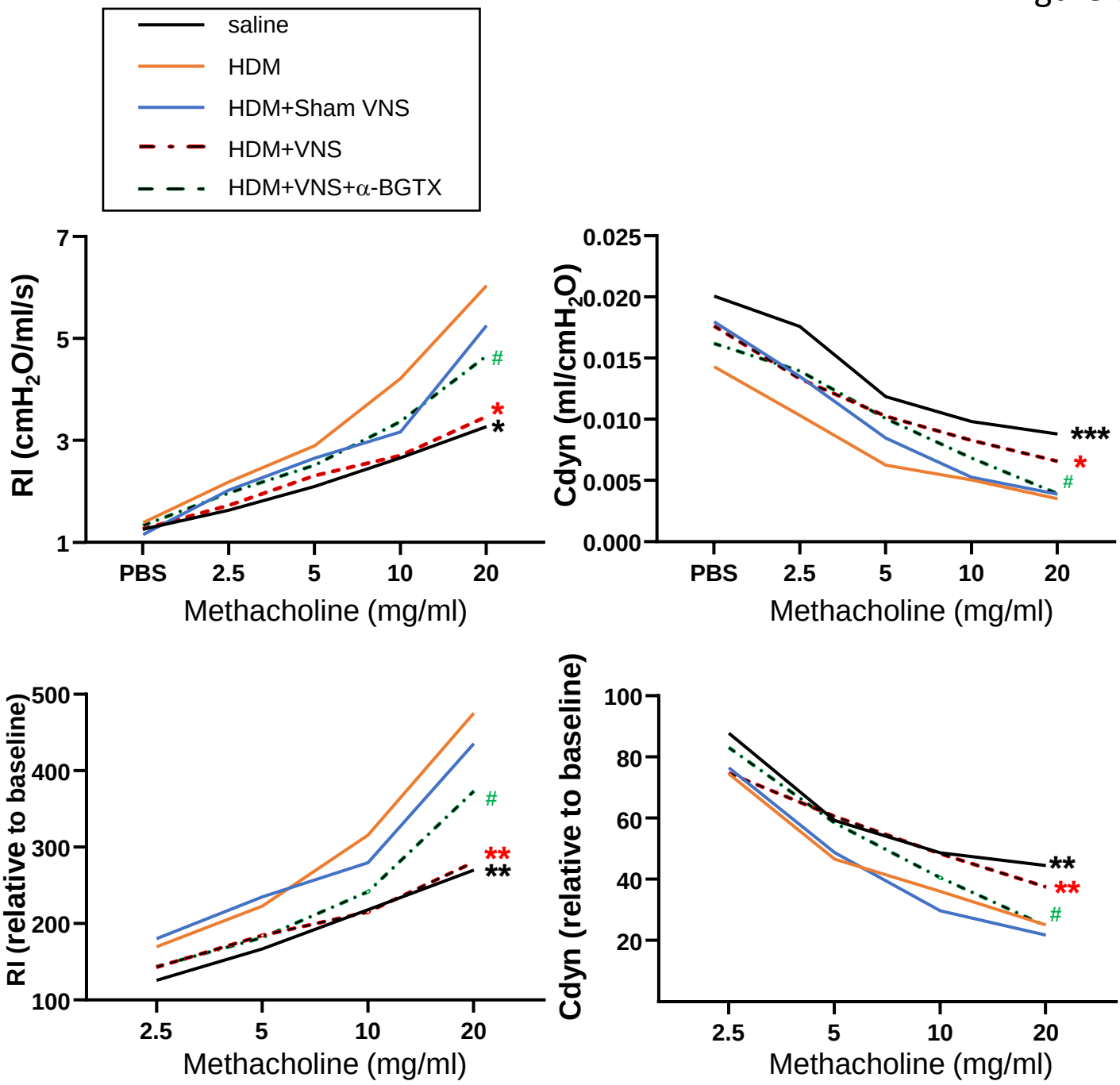
saline
HDM
HDM+Sham VNS
HDM+VNS
HDM+VNS+α-BGTX
RI (cmH2O/ml/s)
7
5
3
1
PBS
2.5
5
10
20
Methacholine (mg/ml)
#
*
*
Cdyn (ml/cmH2O)
0.025
0.020
0.015
0.010
0.005
0.000
***
*
#
RI (relative to baseline)
500
400
300
200
100
**
**
#
Cdyn (relative to baseline)
100
80
60
40
20
**
**
#

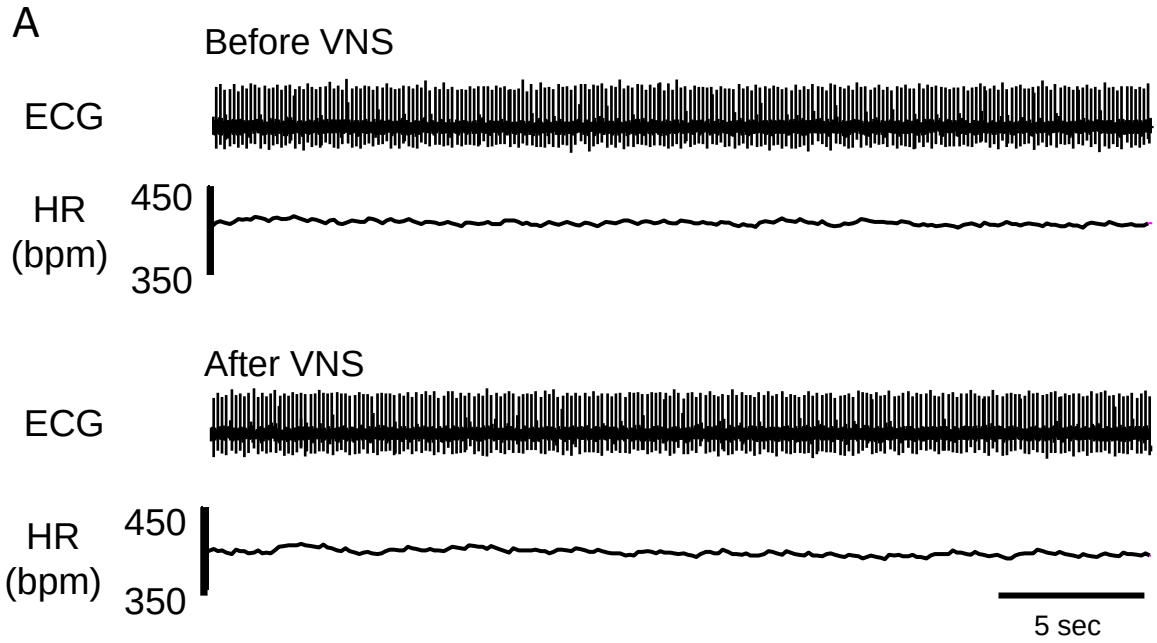
A
Before VNS
ECG
HR
(bpm)
450
350
After VNS
ECG
HR
(bpm)
450
350
5 sec

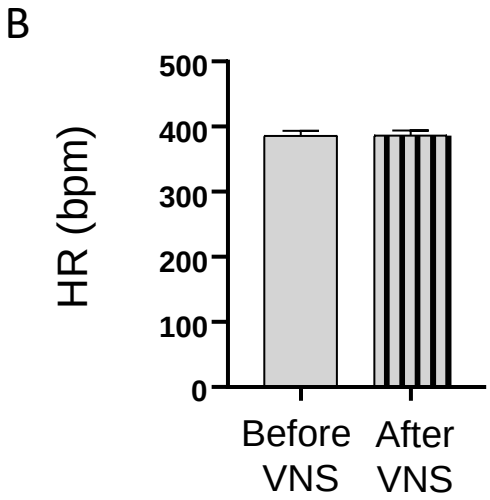
B
HR (bpm)
500
400
300
200
100
0
Before VNS
After VNS

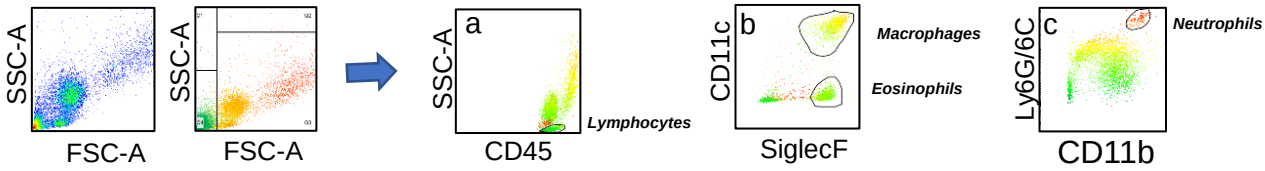
SSC-A
FSC-A
SSC-A
FSC-A
a
SSC-A
CD45
Lymphocytes
b
CD11c
SiglecF
Macrophages
Eosinophils
c
Ly6G/6C
CD11b
Neutrophils